ROYAL SOCIETY
OF CHEMISTRY

PAPER

Check for updates

Oxide anchored multi-charged metal complexes with binary nanoparticles for stable and efficient anti-bacterial coatings on cotton fabrics†

Anjali Nirmala,[ab] Suja Pottath,[bc] Adarsh Velayudhanpillai Prasannakumari,[bd] Valan Rebinro Gnanaraj,[bd] Jubi Jacob,[be] B. S. Dileep Kumar,[be] Saju Pillai, [iD][bc] Rajeev Kumar Sukumaran,*[bd] U. S. Hareesh, [iD] *[bc] Ayyappanpillai Ajayaghosh [iD] *[ab] and Sreejith Shankar [iD] *[ab]

Personal protective equipment (PPE), especially face masks, has received much attention as a quick reaction to pandemic outbreaks to prevent infections caused by airborne microorganisms. Single-use masks are generally made of synthetic polymers such as polypropylene. Discarding the used masks causes serious environmental pollution. Incineration is an energy-intensive process for treating used masks. Therefore, in order to meet the urgent requirement to minimize the use of synthetic polymers in single-use masks, we developed a combination coating comprising of multi-charged metal complexes anchored on TiO_2 and binary nanoparticles containing silver and copper on cotton substrates as anti-bacterial inserts in face masks. The coatings have shown excellent activity against both Gram-negative and Gram-positive bacteria. >99.9% activity against bacteria under standard test conditions and after exposure to extreme conditions of humidity (>90% RH, 45 °C, 6 h), temperature (>110 °C, 6 h), and multiple cycles of washing confirms high anti-bacterial action combined with excellent environmental stability. The combination coatings exhibited excellent activity against bacterial strains that were partially resistant to already proven anti-bacterial agents like silver-copper nanoparticles. With differential partial pressure as low as 1.1 Pa cm^{-2} confirming excellent breathability, good shelf life (exceeding 5 months under ambient conditions), comfort, and cooling effects, these coatings are promising candidates for anti-microbial inserts in cloth-based and otherwise all-polymeric PPE.

1. Introduction

Treatment of infectious diseases has become increasingly challenging due to the emergence of anti-microbial resistance (AMR), which is the leading cause of morbidity and mortality.[1–3] Existing medications and vaccinations may occasionally become ineffective due to the evolution and mutation of causative microbes. Therefore, the development of new and improved chemotherapeutic agents with desired profiles of action has been identified as a prominent vertical in modern treatment modalities.[4] Most of the conventional antimicrobial agents work on the bullet-target principle addressing specific biochemical processes such as enzymatic reactions, transcription, translation, *etc.*, thereby leading to progressive resistance.[5] Notably, during this alarming health crisis, the development of new anti-microbials is struggling to cope with the pace at which AMR is evolving.[5]

Personal protection equipment such as respiratory protective devices (RPDs) including face masks, though aimed at preventing the spread of airborne infectious pathogens, presents several possibilities for microbial transmission.[6] Most of the single-use face masks are generally made of synthetic polymers such as polypropylene and discarding these used masks poses a huge threat to the environment. The commonly employed option of incineration adds exponentially to the cost of managing the waste generated from used masks apart from air pollution. While conventional masks allow for the filtration of microbes to a certain extent, there is no mechanism available

[a] *Chemical Sciences and Technology Division, CSIR-NIIST, Thiruvananthapuram – 695 019, India. E-mail: ajayaghosh@niist.res.in, sreejith.shankar@niist.res.in*

[b] *Academy of Scientific and Innovative Research (AcSIR), Ghaziabad – 201002, India*

[c] *Materials Science and Technology Division, CSIR-NIIST, Thiruvananthapuram – 695 019, India. E-mail: hareesh@niist.res.in*

[d] *Microbial Processes and Technology Division, CSIR-NIIST, Thiruvananthapuram – 695 019, India. E-mail: rajeevs@niist.res.in*

[e] *Agroprocessing and Technology Division, CSIR-NIIST, Thiruvananthapuram – 695 019, India*

for *in situ* disinfection or decontamination. A viable alternative to meet this challenge is to minimize the use of synthetic polymers and substitute the same with reusable cloth-based layers, with the possibility to add-in a replaceable insert of an antimicrobial, filter-efficient, and protective coating. The global antimicrobial coatings market size is projected to grow from USD 12.8 billion in 2023 to USD 30.2 billion by 2030, at a CAGR of 13.07%.[7] Cotton is projected to be the major substrate in the antimicrobial textiles market.[8]

Cotton fabrics provide better air permeability and breathability, softness, comfort, and cooling effect, which make them preferred as the *next-to-skin* textiles.[9] However, natural cotton, under favourable temperature and humidity conditions, provides a hatchery for the rapid proliferation of microorganisms.[10] While personal hygiene by sanitizing and washing are effective against the spread of pathogens, most of these are contingent on human behavior. Therefore, considering the emergence of several pathogenic diseases, improved, cost-effective, and biocompatible antimicrobial agents have to meet an additional challenge of incorporating them in functional coatings, thereby offering a passive solution without the need for constant human interventions. Such approaches have been shown to be effective in preventing the transmission of pathogens *via* contact destruction or disinfection of microbes.

Contact-based destruction of microorganisms requires a favourable interaction of the microbes with surfaces wherein charged species are of particular interest for ensuring microbial surface contact.[11] Multi-charged metal complexes with low toxicity are an emerging class of *metalloantibiotics* having access to different mechanisms of action when compared to conventional antibiotics, which provides a strong case for fighting anti-microbial resistance.[12] Such materials having three-dimensional structural scaffolds[12,13] with inherent antimicrobial properties are of great advantage such that both the anti-microbial effect and charges for surface contact would be warranted by using a single material.[11] The addition of metal nanoparticles with proven anti-microbial activity[14–21] to such coatings not only reduces the amount of such charged materials, wherein the amount of these chemical agents is kept below their toxicity index, but also provides long-lasting, stable, and exceptionally high anti-microbial activity. In this work, we report our efforts towards developing a multi-component coating on cotton fabrics with broad-spectrum anti-bacterial activity, breathability, high shelf-life, low toxicity, and high durability against washing and exposure to temperature and humidity. Though we screened a number of microorganisms in this study, particularly for the multi-charged metal complexes, we report *E. coli* and *S. aureus* as representative Gram-negative and Gram-positive bacteria in the investigations related to the anti-bacterial activity of the coatings. While these coatings are applicable in contact-killing of bacteria and other microorganisms, we envision that the use of such cloth-based layers in personal protection equipment not only adds to *in situ* anti-bacterial activity but also reduces the use of synthetic polymers. Such broad-spectrum anti-microbial coatings are not only useful as inserts in PPE or masks, but also for textile-based applications, barriers for the spread of microbial infections, anti-microbial wipes, *etc.*

2. Experimental section

2.1 Materials and methods

All reagents were used as received without further purification, unless otherwise noted. Syntheses and experiments were carried out in clean and oven-dried glassware. Reactions were monitored using silica gel G-60 F254 aluminum TLC and compounds were visualized by using short/long-wavelength UV lamps. Column chromatography was performed using silica gel 100–200 mesh as a stationary phase.

2.1.1　Molecular characterization. ^{1}H and ^{13}C NMR spectra were recorded in deuterated solvents at 300 K on a 500 MHz (1H) Bruker 109 Advance DPX spectrometer using TMS as an internal standard. Chemical shifts are presented in ppm (δ) along with the corresponding coupling constants (Hz). HRMS data were recorded on a Thermo Scientific Exactive LCMS instrument by the electrospray ionization method with ions given in m/z using an Orbitrap analyser. FT-IR spectra were recorded in the solid state (KBr) using a Shimadzu IRPrestige-21 Fourier transform infra-red spectrophotometer.

2.1.2　Absorption spectroscopy. Electronic absorption spectra in solution were recorded on a Shimadzu UV-2600 spectrophotometer, using a clean and dry Hellma Analytics 10 mm quartz cuvette. Temperature was regulated using a Shimadzu temperature controller and a blank experiment with the corresponding solvent provided the baseline.

2.1.3　Electron microscopy and thermal characterization. TEM images were obtained using a JEOL JEM F200 microscope built with STEM, EDS, and EELS. The samples were dried, redispersed in deionized water using sonication, and drop cast onto carbon-coated copper grids (TED PELLA, INC., 400 mesh) and dried at room temperature for 24 h. SEM micrographs and SEM-energy-dispersive X-ray spectroscopy (SEM-EDS) images of coated cotton fabrics were acquired using a Zeiss EVO 18 Special Edition scanning electron microscope (Carl Zeiss, Germany) equipped with an EDS detection system (Oxford Instruments, X-Max) with an accelerating voltage of 15 kV. Thermogravimetric analyses (TGA) were performed at a heating rate of 10 $^\circ$C min^{-1} under a nitrogen atmosphere using Shimadzu, DTG-60 equipment.

2.1.4　Synthesis. The detailed synthesis procedure and characterization are given in the ESI.† [22]

2.1.5　Cytotoxicity studies. The viability of L6 cells (skeletal muscle cells) was estimated by means of MTT assay[23] using different amounts (1–50 μg) of the parent ligands (**1**, **8**, **L1**, and **L2**) and the metal complexes, **Fe-L1** and **Fe-L2**. The cells, after incubation with the corresponding compound, were washed, and MTT (0.5 g L^{-1}) dissolved in DMEM was added to each well for the estimation of mitochondrial dehydrogenase activity as described previously. After an additional 90 min of incubation at 37 $^\circ$C in a CO$_2$ incubator, 10% SDS in DMSO was added to each of the wells and the absorbance at 570 nm of solubilized MTT formazan products was measured after 45 min, using a micro-plate reader.

2.1.6 Procedure for coating the cotton fabrics. Freshly cut cotton fabric (40 cm × 40 cm) was treated with UV-ozone for 15 min. The metal complex **Fe-L1** or **Fe-L2** (25 mg) was dissolved in acetonitrile (0.5 mL) and was added to TiO_2 sol (2.5 wt%, 100 mL) in water. The mixture was then spray coated (3 layers) using a pressure spray nozzle onto the UV-ozone treated fabric with drying cycles in between. After drying the fabric in a hot air oven at 70 °C, Ag–Cu binary nanoparticle sol was sprayed (3 layers) using the same pressure spray nozzle with drying cycles in between. The coated fabric was dried for 30 min in a hot air oven at 80 °C. Coatings for control experiments were achieved by eliminating the corresponding components using a similar procedure.

2.1.7 Anti-bacterial studies

2.1.7.1 Anti-bacterial investigations of the metal complexes. Bacterial spiking solutions were prepared in Luria Bertani (LB) medium and taken for tests at the 18 h old stage, and diluted as mentioned below, where the colony forming units (CFUs) were approximately 4.3×10^6 and 2.5×10^5 per millilitre for *E. coli* and *S. aureus* respectively (based on CFU counts of the 18 h old sample). The two bacterial suspensions (spiking solutions) of *Escherichia coli* and *Staphylococcus aureus* were serially diluted in sterile saline up to 10^3 and 10^4 respectively. Each of these suspensions was again diluted 10× in saline. The undiluted and diluted suspensions were labelled as 0× and 10×, respectively. Test samples (500 μL) were added to 10 mL of both 0× and 10× dilutions and incubated at 30 °C for one hour at 200 rpm. After incubation, 100 μL samples were taken from both dilutions and spread plated on Luria Bertani agar plates and incubated at 37 °C for 24 h. After 24 h of incubation, the plates were observed for colony formation and counted where applicable. Efficacies were calculated as % reduction of CFUs from the original counts in the spiking solution.

The broad-spectrum anti-bacterial action of the complexes **Fe-L1** and **Fe-L2** against different bacteria was investigated using the disc diffusion method. *Bacillus cereus* MTCC 1305 and *Mycobacterium smegmatis* MTCC 993 were chosen as Gram-positive models and *Escherichia coli* MTCC 2622, *Klebsiella pneumoniae* MTCC 109, and *Pseudomonas aeruginosa* MTCC 2642 were chosen as Gram-negative strains. The test bacteria were first inoculated separately in nutrient broth and incubated at 37 °C for 18 h. Each of the inocula was then adjusted to 0.5 McFarland turbidity standards and swabbed into Mueller–Hinton plates. A 10 mg mL^{-1} stock solution of the metal complex **Fe-L1** or **Fe-L2** was prepared in DMSO and 30 μL from the stock solution was loaded onto 6 mm sterile discs. The addition of DMSO alone served as control and similar solutions prepared from the bipyridines **1** and **8** and the ligands **L1** and **L2** were used for comparison. Plates were incubated for 24 h at 37 °C and the zone of inhibition was measured.

2.1.7.2 Anti-bacterial investigations of the coatings

AATCC 147 test (parallel streak method). The test bacteria (*Staphylococcus aureus* and *Escherichia coli*) were prepared in a liquid culture medium. Bacterial spiking solutions were prepared in Luria Bertani (LB) medium and taken for test at the 18 h old stage and were diluted appropriately using sterile saline to get a final concentration of $\sim 10^4$ CFUs per mL. One loopful of the diluted inoculum suspension was used to streak 5 consecutive, evenly spaced parallel streaks onto the solidified LB agar plates. The streaks were intentionally varied in the concentration of the bacteria. Anti-bacterial agent-coated strips (25 mm × 50 mm) were carefully placed on the LB agar surface aseptically, over the parallel streaks. A parallel untreated cotton fabric was also tested as control. The contact of the cotton fabric and the inoculated agar was ensured by applying even gentle pressure on the sample. The plates were incubated for 24 h at 37 °C. Each experiment was performed in triplicate. Positive controls using ampicillin- or penicillin/streptomycin-coated cotton fabric of the same size were also tested.

ASTM E2149-13a test. This test determines the quantitative anti-microbial activity of a coating by shaking it with a concentrated bacterial suspension for a 1 h contact time. The suspension is then serially diluted before and after contact and cultured. The number of viable organisms from the suspension is determined and the percent reduction is calculated by comparing with controls. In a typical experiment, coated cotton pieces (weight = 1 ± 0.1 g) were added to a bacterial inoculum (50 ± 0.5 mL) and shaken for a 1 h contact time. The bacterial suspensions were then serially diluted and cultured on pre-prepared agar plates. Filtration may be required if any sort of degradation is suspected. The plates were then incubated for 24 h at 37 °C. After 24 h of incubation, the plates were observed for colony formation and counted where applicable. Efficacies were calculated as % reduction of CFUs from the original counts in the spiking solution, before adding the coatings. Residual bacterial retention on the coatings was tested using agar imprint tests.

2.1.7.3 SEM imaging of anti-bacterial action. The morphological alterations in bacterial cell walls caused by the metal complexes **Fe-L1** and **Fe-L2** were monitored by SEM analysis. Strains of *Mycobacterium smegmatis* MTCC 993 and (D–F) *Pseudomonas aeruginosa* MTCC 2642 were chosen as representative examples. After the treatments as described in Section 5.2 (disc diffusion method), the pellets were washed with phosphate-buffered saline (PBS) and centrifuged (8000 rpm) for 5 min. The pellets were immediately fixed with 2% glutaraldehyde (v/v) at 4 °C for 12 h. The bacterial suspension was again centrifuged (5000 rpm for 5 min). Then the supernatant was removed and washed three times with PBS to remove any trace of glutaraldehyde. The pellets were then post-fixed in 1% (w/v) osmium tetroxide at 4 °C for 1 h and washed twice with PBS. The samples were dehydrated in graded ethanol series (30, 50, 70, 80, 95 and 100%) for 10 min each. A few drops of the bacterial suspensions were drop-cast on aluminium foil attached to conductive carbon tape and dried in sterile airflow. The samples were sputtered with gold to avoid charging and analysed under 10 kV in a scanning electron microscope.

2.1.7.4 Stability studies on the coatings. In order to test the stability of the coatings towards humidity and temperature, the

coated cotton fabrics were kept at 90–95% relative humidity (45–50 °C) or 110 °C for six hours. The retention of anti-bacterial activity was then investigated using AATCC 147 or ASTM E2149-13a tests. The stability of the coatings towards washing was investigated under ISO 6330 specifications (2 kg textile with 20 g detergent, 40 °C, agitation for 35 min). In a typical experiment, 3.7 g of the coated cotton fabric was added to a container with 38 mg of detergent and 500 mL of water. The system was subjected to vigorous stirring for 35 min at 40 °C. The fabric was then retrieved and dried in a hot-air oven at 80 °C. The retention of the anti-bacterial activity of the dried fabric was then investigated using AATCC 147 or ASTM E2149-13a tests. The washing–drying cycle was repeated multiple times (5×). The as-coated sample, without any treatment, served as the control.

2.1.7.5 Determination of MIC. The broth micro-dilution-based MIC determination experiments were conducted according to EUCAT guidelines. The experiments were conducted in 96 well plates, where each well was supplemented with a different concentration of test compounds **Fe-L1** and **Fe-L2** in a total volume of 200 μL of sterile MHB (Muller Hinton Broth) cation-adjusted medium (pH 7.2). Diluted test cell cultures (2 μL) of 0.05 OD adjusted ($\sim 5 \times 10^5$ CFU per mL) overnight grown cultures of *E. coli*, *S. aureus*, *M. smegmatis*, and *K. pneumonia* were used for the studies. Experiments without the test compounds and without bacterial inoculum served as negative controls. In addition, two known antibiotics (ampicillin and gentamycin) with known MIC were used as positive controls. The cultures were incubated at 37 °C for 18 h, and then OD_{600} was measured. The growth inhibition was assessed in comparison with a negative control. The MIC was determined as the test compound concentration that inhibited more than 90% of cell growth based on the OD_{600} measurements. All the experiments were conducted with biological duplicates.

2.1.7.6 Live–dead assays

Preparation of live and dead cultures. Live and dead culture assays were performed using a BacLight Kit (Invitrogen, 2004). Turbid overnight grown test cultures in LB medium were collected in microfuge tubes, and centrifuged at 5000 rpm for 5 min, at 25 °C. The pellets were re-suspended in 0.85% saline, and the above steps were repeated twice to remove completely the media components and other particles in the medium. After washing cycles, the cells were suspended in 300 μL of saline, and were equally distributed in three microfuge tubes. One tube was kept as control. **Fe-L1** and **Fe-L2** at their MIC were added to the remaining two tubes and incubated for 20 mins. After incubation, the cells were washed thrice (with saline), and finally re-suspended in 50 μL of saline.

Staining samples with SYTO 9 and PI. Stock solutions of SYTO 9 and PI were prepared in 1 : 2 ratios respectively, where 1 μL of SYTO 9 and 2 μL of PI were suspended in 497 μL of 0.85% saline in microfuge tubes. The tubes were then covered with aluminum foil, and were stored on ice. Both the control and treated samples were stained by adding 50 μL of the dye

solutions. This stained mixture was incubated in the dark for 30 min at room temperature. The dye-mixed samples were then washed thrice to remove any excess dye. Finally, the stained samples were suspended in 50 μL of 0.85% saline and the stained cells were viewed under a fluorescence microscope under transluminescence, at 515 nm (GFP) and 610 nm (RFP).

2.1.7.7 Quantification in live–dead assays. The number of viable cells recovered from the MIC-treated samples was estimated from the number of colony forming units (CFUs). The CFUs were estimated using a spot assay agar plating method. 20 μL samples collected from both overnight (~ 18 h) incubated control and **Fe-L1** or **Fe-L2** treated wells were serially diluted in 180 μL of sterile 0.85% saline. The serial dilution was done up to 10^8 times. 20 μL samples from 10^8, 10^6, and 10^4 dilutions were spotted onto LB agar plates and were incubated at 37 °C overnight. The number of viable colonies was estimated and compared with controls.

3. Results and discussion

A large number of reports on using different strategies to improve the anti-microbial properties of natural cotton have emerged over the years.[24–27] Nanoparticles of metals such as silver and copper, and oxides of transition metals such as titanium and zinc have been extensively used for imparting anti-microbial properties to different substrates.[14–21,28,29] Such nanocrystalline components with inherent anti-microbial action are essential components of bandages, ointments, and catheters. However, several recent studies have shown increasing anti-microbial resistance to these materials.[30–34] The corresponding ionic species leaching from the nanoparticles are believed to be among the most active anti-microbial agents.[14–21,28,29] The reduction of these ions to the metal species at zero oxidation state *via* the production of redox-active metabolites or mutations combined with other mechanisms in microorganisms tends to shut down the anti-microbial action, leading to resistance.[30–33] Therefore, a combination of multiple components having inherent anti-microbial activity is most likely the best strategy for achieving efficient protective coatings against pathogens wherein the adverse effects of AMR and toxicity could be resolved to a greater extent.[34–36]

To this end, we envisaged the synthesis of dual-active multi-charged bipyridine-based metal complexes **Fe-L1** and **Fe-L2** with inherent anti-bacterial properties. These complexes having multiple positive charges with their possible ion-pairing ability and electrostatic interactions allow better microbial surface contact, thereby inducing higher chances for contact killing of pathogens.[37,38] We have earlier reported a series of bipyridine- and terpyridine-based metal complexes for smart applications and energy storage.[39–45] A base coat of nanocrystalline TiO_2 anchored the metal complexes onto the cotton substrates using a simple spray coating process. A subsequent spray of freshly prepared binary particles of chitosan-stabilized Ag–Cu nanoparticles[46,47] ensured excellent anti-bacterial activity. The combination of **Fe-L**@TiO_2 and chitosan-capped Ag–Cu NPs
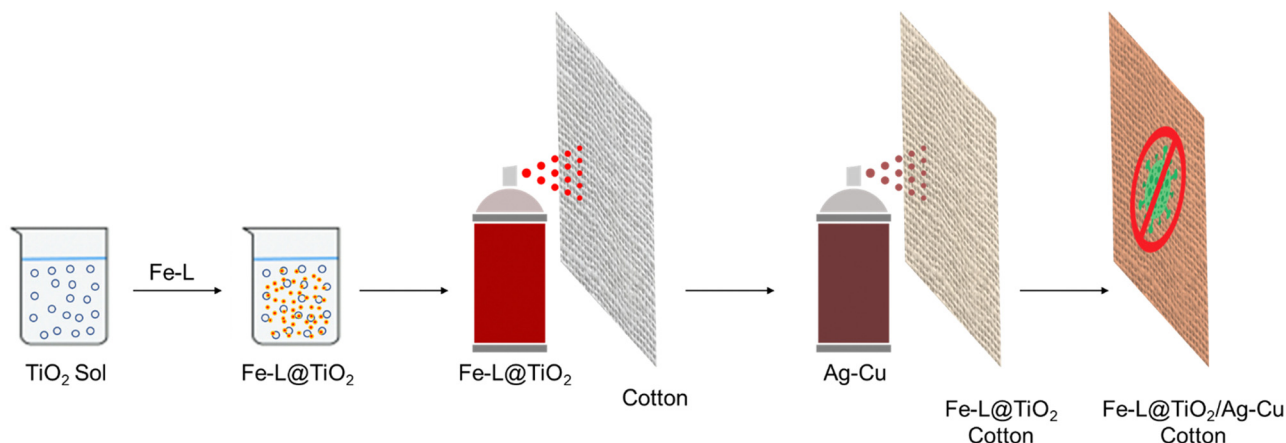
Fig. 1 Schematic representation of the anti-microbial coating process on cotton fabrics. 25–50 mg of the metal complex **Fe-L** was dissolved in acetonitrile (0.5 mL) and was added to a 2.5 wt% TiO_2 sol (100 mL) in water. The mixture was spray coated (3 layers) using a pressure spray nozzle onto a UV-ozone-treated fabric (40 cm × 40 cm) with drying cycles in between. After drying the fabric in a hot air oven at 70 °C, Ag–Cu binary nanoparticle sol was sprayed (3 layers) with drying cycles in between. The coated fabric was dried for 30 min in a hot air oven at 80 °C.

fortifies better activity at low mass loading combined with high environmental stability, shelf-life, and low toxicity (Fig. 1).

Synthesis and characterization of Fe-L

The ligands **L1** and **L2** were synthesized from the corresponding commercially available 2,2′-bipyridine derivatives **1** and **8**, respectively (Schemes S1 and S2, ESI†).[45] Stirring the methanolic solutions of ligands **L1** and **L2** with $FeCl_2 \cdot 4H_2O$ in a 1.5 : 1 molar ratio, with occasional heating to 50 °C over 12 h, followed by precipitation from saturated KPF_6 (aq.) solution afforded the metal complexes **Fe-L1** and **Fe-L2** in near quantitative yields (Schemes S3 and S4, ESI†).[43–45] The synthetic procedure and characterization data are detailed in the Experimental section. The formation of the metal complexes was confirmed by the emergence of an MLCT band (538 nm for **Fe-L1** and 533 nm for **Fe-L2**) corresponding to a reddish color (Fig. S1, ESI†). FT-IR spectra confirmed that all the structural features of the ligands **L1** and **L2** were preserved in the corresponding complexes. Since the ligands and the metal complexes have multiple positive charges, they were precipitated from their aqueous solutions as their PF_6 salts. The presence of PF_6 anions was confirmed from the strong peaks at 555 cm^{-1} ($\delta(PF_6)$ bending vibrations, sharp) and 804–816 cm^{-1} (stretching vibrations of the PF_6 anion). The peak at 804 cm^{-1} for **L1** and **L2** was found to be shifted to 816 cm^{-1} for the metal complexes along with concomitant sharpening. The peak corresponding to C–N stretching vibrations was found at 1169 cm^{-1} for all the compounds. The CH_2 bending vibrations for the metal complexes were found to be shifted by 7 cm^{-1} (1453 cm^{-1}) as compared to the ligands (1445 cm^{-1}), while the C–H bending peak was observed at 1476 cm^{-1} for all the compounds. Characteristic peaks corresponding to C_{ar}–C_{ar} were also found to be slightly shifted for the metal complexes (1506 cm^{-1}) as compared to **L1** and **L2** (1509 cm^{-1}). The C=C and C=N stretching vibrations were also confirmed by the presence of the peaks at 1642 cm^{-1} in the corresponding FT-IR spectra (Fig. S2, ESI†).

Cytotoxicity studies of the metal complexes

One of the prerequisites for using metal–organic complexes as anti-bacterial agents in a coating is to ensure low cytotoxicity to healthy cells. The viability of L6 cells (skeletal muscle cells) was estimated by means of MTT assay[23] using different amounts (1–50 μg) of the parent ligands and the metal complexes, **Fe-L1** and **Fe-L2**. The cells, after incubation with the corresponding compound, were washed, and MTT (0.5 g L^{-1}), dissolved in DMEM, was added to each well for the estimation of mitochondrial dehydrogenase activity as described previously. After an additional 90 min of incubation at 37 °C in a CO_2 incubator, 10% SDS in DMSO was added to each of the wells and the absorbance at 570 nm of solubilized MTT formazan products was measured after 45 min, using a micro-plate reader. The results confirmed that the metal complexes (**Fe-L1** and **Fe-L2**) exhibited much less cytotoxicity when compared to the parent ligands (**L1** and **L2**) and the corresponding 2,2′-bipyridines (**1** and **8**). **Fe-L1** and **Fe-L2** exhibited >90% cell viability after 24 h of incubation with L6 cells (Fig. 2).

Antimicrobial studies of the metal complexes

The metal complexes **Fe-L1** and **Fe-L2** were designed to have multiple charges to ensure microbial contact with the
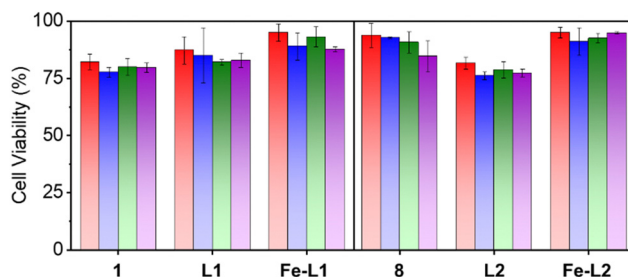

Fig. 2 Cell viability data for the bipyridines (**1** and **8**), ligands (**L1** and **L2**) and the metal complexes (**Fe-L1** and **Fe-L2**). Color codes: red: 1 μg, blue: 10 μg, green: 25 μg, and purple: 50 μg.

substrates. Several prior reports have proposed the use of metal complexes as anti-microbial agents. We, therefore, explored the broad spectrum anti-bacterial action of these complexes against different bacteria using the disc diffusion method. *Bacillus cereus* MTCC 1305 and *Mycobacterium smegmatis* MTCC 993 were chosen as Gram-positive models and *Escherichia coli* MTCC 2622, *Klebsiella pneumoniae* MTCC 109, and *Pseudomonas aeruginosa* MTCC 2642 were chosen as Gram-negative strains.

The test bacteria were first inoculated separately in nutrient broth and incubated at 37 °C for 18 h. Each of the inocula was then adjusted to 0.5 McFarland turbidity standards and swabbed into Mueller–Hinton plates. A 10 mg mL^{-1} stock solution of the metal complex **Fe-L1** or **Fe-L2** was prepared in DMSO and 30 µL from the stock solution was loaded onto 6 mm sterile discs. The addition of DMSO alone served as control and similar solutions prepared from the bipyridines **1** and **8** and the ligands **L1** and **L2** were used for comparison. Sterile discs loaded with the agents were placed on separate plates and pre-inoculated with each tested culture, the plates were then incubated for 24 h at 37 °C and the zone of inhibition was measured. Both **Fe-L1** and **Fe-L2** were found to exhibit significant anti-bacterial activity against all test organisms, with a zone of inhibition up to 22 mm (Table 1). The activity of the metal complexes was superior to the parent compounds in most cases (Fig. 3 and Fig. S3, ESI†). The low cytotoxicity combined with good anti-bacterial activity makes this class of molecules interesting for investigation as new *metalloantibiotics*.[12]

While the exact mechanism of action of these metal complexes is not yet fully understood, the unique anti-microbial mechanisms that metal complexes exhibit include ROS generation, redox activation, ligand exchange or release, and catalytic generation of toxic species or depletion of essential substrates.[12] Therefore, complexation with transition metals has also been evidenced as a strategy to improve the antimicrobial activity of several organic drugs.[37] Scanning electron microscopy illustrated the effect of **Fe-L1** and **Fe-L2** on bacterial cell membranes (Fig. 4). Compared to control, partial to complete membrane lysis was obtained when **Fe-L1** and **Fe-L2** were used as anti-bacterial agents. As shown in prior reports, the multi-charged metal complexes most likely adsorb onto the cell walls *via* electrostatic interactions and damage the cell walls leading to cell death.[37] Live and dead culture assays (BacLight Kit, Invitrogen,
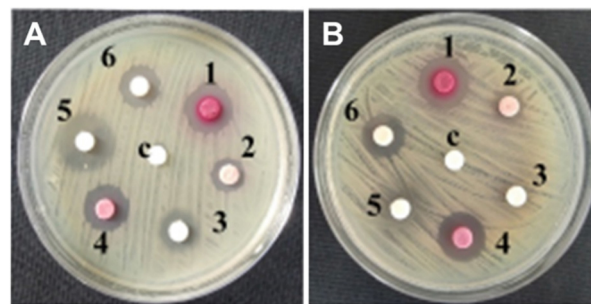

Fig. 3 Anti-bacterial activity of the compounds used in this study against (A) *Mycobacterium smegmatis* MTCC 993 and (B) *Klebsiella pneumoniae* MTCC 109. The compounds are numbered as follows: 1: **Fe-L1**, 2: **L1**, 3: bipyridine **1**; 4: **Fe-L2**, 5: bipyridine **8**, and 6: **L2**. One Gram-positive and one Gram-negative bacteria are shown as representative examples. See ESI† (Fig. S3) for the data on other strains.

2004) performed against different bacterial strains further confirmed the anti-bacterial activity of the metal complexes **Fe-L1** and **Fe-L2** (Fig. S4–S6, ESI†).

The antibiotic susceptibility test and MIC profile examination were performed according to the EUCAT standard antibiotic susceptibility test (AST) method (Table S1, ESI†). Exposure to both **Fe-L1** and **Fe-L2** resulted in more than 4 log reduction in viable cell counts, which indicates that the organisms are susceptible to these compounds (Table S2, ESI†). The test pathogenic strains showed phenotypic susceptibility to **Fe-L1** and **Fe-L2**, with MIC values of 4.3 µg mL^{-1} and 8.4 µg mL^{-1}, respectively. The MIC values are comparable to those of the clinically relevant antibiotics ampicillin and gentamycin. While ampicillin was found to be active against Gram-negative *K. pneumoniae* MTCC 109 (MIC 2 µg mL^{-1}), and was not effective against other strains at the tested MIC concentration (8 µg mL^{-1}), gentamycin was found to be effective at an MIC range of 2–4 µg mL^{-1} against the tested strains.

Multi-component coatings on cotton fabrics

Though we identified new multi-charged metal complexes as dual-active anti-bacterial agents capable of ensuring microbial surface contact, dip-coating a solution of **Fe-L1** and **Fe-L2** did not result in stable coatings on cotton fabrics. One possible strategy to anchor the metal complexes onto the fibres of cotton fabrics is to use a surface-adhering base-coat of a

Table 1 Anti-bacterial performance of the compounds used in this study[a]

| S. no. | Compound | Zone of inhibition (mm) | | | | |
		E. coli	*M. smegmatis*	*P. aeruginosa*	*K. pneumoniae*	*B. cereus*
1	**Fe-L1**	10.33 ± 0.57	18.33 ± 0.57	20 ± 0	17 ± 0	22 ± 0
2	**L1**	0	12 ± 0	15 ± 0	10 ± 0	15 ± 0
3	**1**	0	10 ± 0	10 ± 0	0	13 ± 0
4	**Fe-L2**	12 ± 0	16 ± 0	18 ± 0	17 ± 0.57	16.33 ± 0.57
5	**8**	10 ± 0	15 ± 0	20 ± 0	10 ± 0	20 ± 0
6	**L2**	0	14.33 ± 0.57	15 ± 0	15 ± 0	15 ± 0
Control	DMSO	0	0	0	0	0

[a] The entries without errors (standard deviation) gave consistently similar values for experiments done in triplicate. The standard deviation was typically less than 0.1 mm in these experiments.
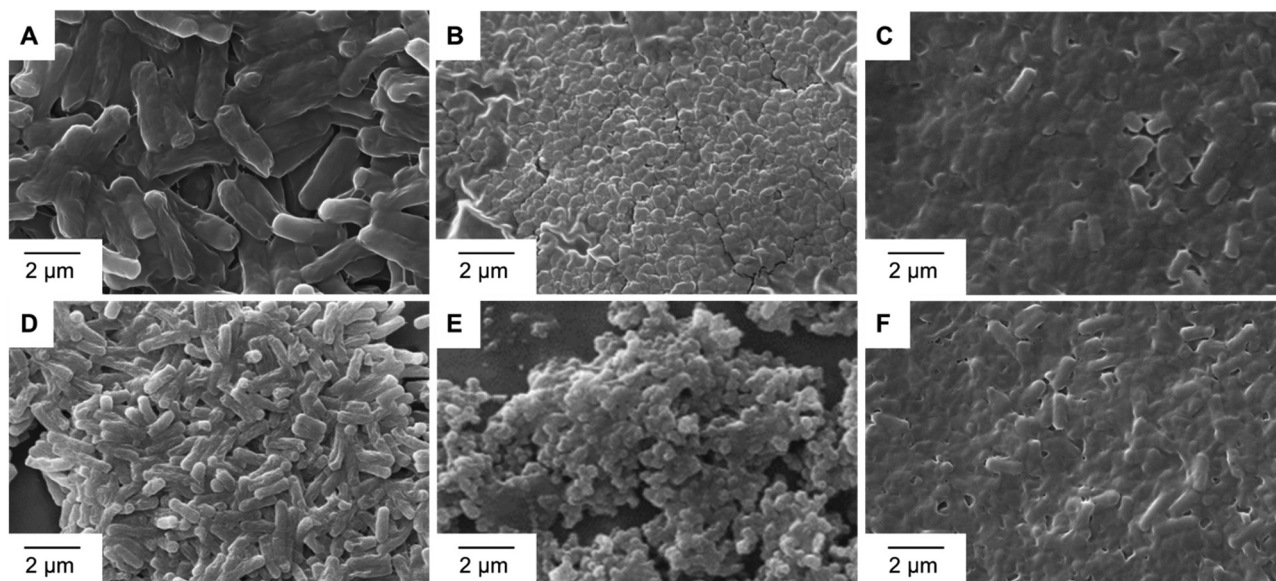
Fig. 4 SEM images of (A)–(C) *Mycobacterium smegmatis* MTCC 993 and (D)–(F) *Pseudomonas aeruginosa* MTCC 2642, (A) and (D) before (control) and after incubation with (B) and (E) **Fe-L1** and (C) and (F) **Fe-L2**, showing cell membrane lysing.

non-interfering material. In this context, nanocrystalline TiO_2 and its composites have proven to have anti-microbial properties and negligible cytotoxicity with surface anchoring hydroxy groups which are available to bind onto suitable surfaces.[48–50] Therefore, we adsorbed **Fe-L1** and **Fe-L2** on TiO_2 nanoparticles to strongly adhere the metal complexes to the fibres of cotton fabrics.

A freshly cut piece of cotton fabric (40 cm × 40 cm) was treated with UV-ozone for 15 min. A sol of TiO_2 (100 mL) was freshly prepared in water. **Fe-L1** or **Fe-L2** (25 mg) was dissolved in acetonitrile (0.5 mL) and was added to the TiO_2 sol and mixed well. The mixture was then spray coated using a pressure spray nozzle onto the UV-ozone treated fabric and then dried using a flow of hot air. This procedure was repeated three times to form a 3-layer coating of the base coat, **Fe-L@TiO₂** (Fig. 1). The modified fabric was then dried in a hot-air oven at 70 °C. Meanwhile, Ag–Cu binary nanoparticles (Fig. S7, ESI†) were synthesized (microwave, 900 W, 3.5 min) from equimolar solutions of silver nitrate (100 mL) and copper nitrate (100 mL) in the presence of chitosan (3% w/v, 200 mL) and ascorbic acid (10% w/v, 20 mL) in water. The reaction was then carried out under microwave at a power of 900 W for 3.5 min. Metal nanoparticles, particularly silver (Ag) and copper (Cu), have been shown to have efficient anti-microbial properties against different pathogenic microorganisms.[12,51,52] The Ag–Cu nanoparticle sol was then spray-coated onto the dried cotton fabric modified with the base coat using the same pressure spray nozzle. Three layers of the bimetallic NPs were sprayed with drying cycles in between by a procedure similar to that for the base coat (Fig. 1). The coated fabric was then dried for 30 min in a hot air oven at 80 °C (Fig. S8, ESI†). The final coating therefore had three layers of the **Fe-L@TiO₂** base-coat over which three layers of bimetallic Ag–Cu NPs were coated. The anti-microbial activity of the combination **Fe-L@TiO₂/Ag–Cu** (L = **L1** or **L2**) was also tested against *Staphylococcus aureus* and *Escherichia coli* (Fig. S9, ESI†).

TEM images of redispersed binary Ag–Cu nanoparticles confirmed a broad size distribution (40–200 nm, Fig. S7, ESI†). As expected, the sequential spray process resulted in the modification of the cotton fibres without blocking the pores which was clearly evident from scanning electron microscope images (Fig. S10, ESI†). It is indeed a significant attribute to have unblocked pores for low differential partial pressure and hence better breathability. The differential partial pressure was obtained in the order of 1.1 Pa cm^{-2} at 65 ± 2% relative humidity and 21 ± 1 °C temperature, which is less than the prescribed limits, to ensure good breathability prospects.[53–55] The presence of all the elements and their uniform distribution in coated fabrics were qualitatively confirmed by energy dispersive X-ray analysis (EDX) on SEM (Fig. S11–S16, ESI†). Thermogravimetric analysis of the coated fabrics showed good thermal stability until 200 °C (Fig. S17, ESI†). The amount of Ag–Cu in the coating was found to be 0.3 and 0.4 wt%, which is below the toxicity index of these metal nanoparticles (Table S3, ESI†).[12]

Anti-bacterial studies on cotton fabrics

In an attempt to test our hypothesis of combining cationic metal complexes with binary metal nanoparticles for efficient anti-bacterial action, the coated fabrics were tested under AATCC-147 and ASTM-E2149-13a standards. The parallel streak method (AATCC-147) confirmed the excellent anti-bacterial activity of **Fe-L@TiO₂/Ag–Cu** (L = **L1** or **L2**) modified cotton fabrics against representative Gram-positive (*Staphylococcus aureus*) and Gram-negative (*Escherichia coli*) bacteria. The anti-bacterial activity of the coated cotton fabrics (Fig. 5E and F) was found to be either similar or superior to that of positive controls using ampicillin- (Fig. 5A and B) or penicillin/streptomycin-coated cotton fabric (Fig. 5C and D) of the same size.
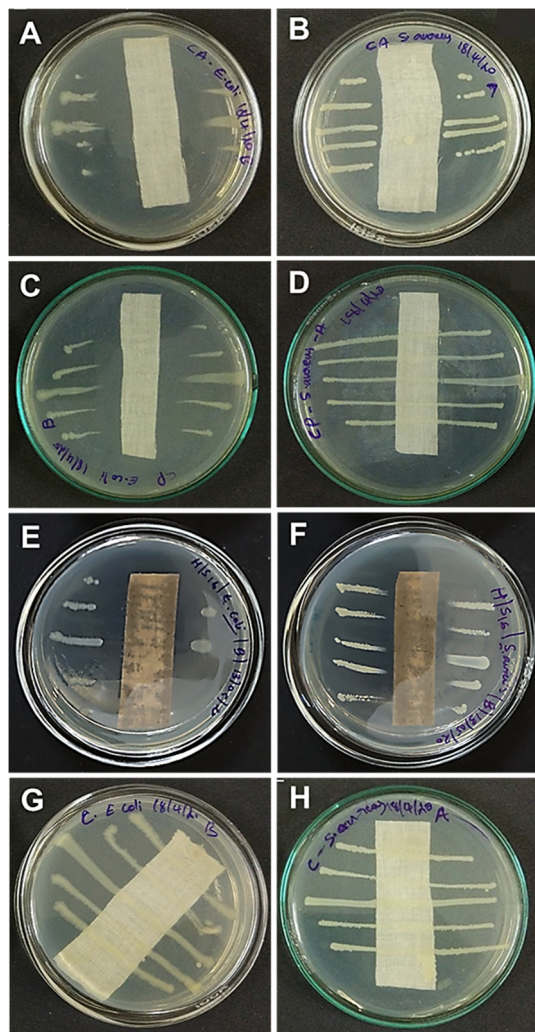
Fig. 5 Antimicrobial activity of (A) and (B) ampicillin-coated, (C) and (D) penicillin/streptomycin-coated, and (E) and (F) **Fe-L1**@TiO$_2$/Ag–Cu-coated cotton fabrics and (G) and (H) pristine cotton fabrics (control) against (A), (C), (E), and (G) *Escherichia coli* and (B), (D), (F), and (H) *Staphylococcus aureus*, tested under AATCC-147 standards.

Penicillin/streptomycin combination was indeed not effective against *Staphylococcus aureus* (Fig. 5D). The quantitative adsorption tests using ASTM-E2149-13a under dynamic contact conditions corroborated the complete bacterial disinfection capabilities of **Fe-L**@TiO$_2$/Ag–Cu (L = **L1** or **L2**)-coated cotton substrates (Fig. S18, ESI†).

In order to establish the superior properties of the combination coating, control experiments were conducted using cotton fabrics coated with individual components and partial combinations of the components. While coatings of **Fe-L** (L = **L1** or **L2**), TiO$_2$, or Ag–Cu NPs alone were completely unstable, **Fe-L**@TiO$_2$/Ag–Cu (L = **L1** or **L2**)-coated cotton substrates exhibited excellent environmental stability. Furthermore, the anti-bacterial activity of coatings fabricated from the individual components was also not satisfactory (Fig. S19, ESI†). Though the anti-microbial effects of Ag, Cu, and Ag–Cu are well documented in the literature,[12,51,52] using a different base-coat instead of **Fe-L**@TiO$_2$ (L = **L1** or **L2**) also resulted in diminished anti-bacterial activity of Ag–Cu-coated cotton substrates (Fig. S20, ESI†). These results demonstrate the significance and synergistic effect of different components in **Fe-L**@TiO$_2$/Ag–Cu (L = **L1** or **L2**) in imparting excellent anti-bacterial activity to the coatings. Moreover, the use of water-based sprays benefits from facile wettability of cotton substrates.

The stability and shelf-life of anti-microbial coatings are crucial parameters that determine their application under real-world conditions. No detectable decrease in activity was observed for **Fe-L**@TiO$_2$/Ag–Cu (L = **L1** or **L2**)-coated cotton fabrics kept under ambient conditions for more than 20 weeks, confirming their excellent shelf-life. The coated fabrics were exposed to temperatures exceeding 110 °C or >90% relative humidity at 45–50 °C for more than 6 h. These extreme conditions did not affect the anti-bacterial activity of the substrates and complete bacterial disinfection was observed for the exposed cotton fabrics (Fig. S21, ESI†). On the other hand, the absence of the **Fe-L**@TiO$_2$ (L = **L1** or **L2**) base-coat resulted in low anti-bacterial activity, which further subsided after exposure to high temperature and humidity (Fig. S22, ESI†). **Fe-L**@TiO$_2$/Ag–Cu (L = **L1** or **L2**)-coated cotton fabrics were also found to be resistant to multiple washing under ISO 6330 specifications (2 kg textile with 20 g detergent, 40 °C, agitation for 35 min). Complete bacterial disinfection was observed for coated fabrics after subjecting them to a series of 5–10 washing/drying cycles (Fig. S23, ESI†). Coatings fabricated from individual components or their partial combinations were leached off after 1–2 cycles of washing, even in the absence of detergents.

The excellent anti-bacterial properties of the **Fe-L**@TiO$_2$/Ag–Cu (L = **L1** or **L2**)-coated cotton fabrics combined with high environmental stability make these coatings versatile enough to be used as replaceable inserts in face masks. Recent experiments using **Fe-L**@TiO$_2$/Ag–Cu (L = **L1** or **L2**) have also shown promising activity against fungal, yeast, and spore models, confirming broad-spectrum anti-microbial activity. Since multiple washing or heat treatment does not alter the anti-bacterial properties of the coated cotton fabrics, they can be reused after washing. The presence of photocatalytically active TiO$_2$ also favours light-induced degradation and removal of organic remnants. While a number of reports on antibacterial fabrics are available in the literature, stable and efficient anti-microbial action of modified natural cotton or nanofibrous membranes has been the subject of extensive investigations. Commendable progress has also been made in terms of activity, stability, and biocompatibility of these coatings.[56–58] We believe that the use of such coatings imparts an *in situ* disinfection mechanism that is otherwise absent in conventional PPE.

4. Conclusions

Cloth-based layers provide an alternative to all-polymeric PPE, whereby the amount of synthetic polymers can be reduced

leading to better environmental sustainability. The cotton-based anti-bacterial inserts developed in this study provide a reliable case for the use of self-disinfecting inserts as an additional layer of protection in face masks and other PPE. While the filtration efficiency of cotton-based inserts is known to be low, a combination of non-woven PP-based layers sandwiching the cotton-based anti-microbial inserts is probably the best approach towards efficient anti-microbial masks with reduced amounts of synthetic polymers. The combination coating combines contact-based destruction of microbes with multiple mechanisms arising from the synergistic action of different components. While this strategy allows maintaining each component of the combination below toxicity levels, we believe that such combination techniques will also assist in combating the emergence of anti-microbial resistance.

Author contributions

AN and SP carried out the synthesis and characterization of all the compounds and materials. AVP, VRG, JJ, and BSDK carried out the anti-bacterial analysis. SS and USH fabricated the coatings. SP carried out SEM imaging and EDS. RKS, USH, AG, and SS conceptualized and supervised the project. AN, SP, SP, RKS, USH, AA, and SS wrote the manuscript. RKS, USH, AA, and SS reviewed and edited the manuscript. All authors approved the submission of the reviewed draft.

Conflicts of interest

There are no conflicts to declare.

Acknowledgements

Notes and references

1 E. M. Darby, E. Trampari, P. Siasat, M. S. Gaya, I. Alav, M. A. Webber and J. M. A. Blair, *Nat. Rev. Microbiol.*, 2023, **21**, 280–295.

2 D. G. J. Larsson and C.-F. Flach, *Nat. Rev. Microbiol.*, 2022, **20**, 257–269.

3 C. J. L. Murray, K. S. Ikuta, F. Sharara and L. Swetschinski, *et al.*, *Lancet*, 2022, **399**, 629–655.

4 M. S. Butler, V. Gigante, H. Sati, S. Paulin, L. Al-Sulaiman, J. H. Rex and P. Fernandes, *Antimicrob. Agents Chemother.*, 2022, **66**, e0199121.

5 B. Sharma, S. Shukla, R. Rattan, M. Fatima, M. Goel, M. Bhat, S. Dutta, R. K. Ranjan and M. Sharma, *Int. J. Biomater.*, 2022, 6819080.

6 A. Tuñón-Molina, K. Takayama, E. M. Redwan, V. N. Uversky, J. Andrés and Á. Serrano-Aroca, *ACS Appl. Mater. Interfaces*, 2021, **13**, 56725–56751.

7 Source: Precedence Research, https://www.precedenceresearch.com/antimicrobial-coatings-market.

8 Source: Global Insights, https://www.gminsights.com/industry-analysis/antimicrobial-textiles-market.

9 Z. Li, Y. Zhang, W. Xia, Y. Tanga and Q. Li, *Mater. Adv.*, 2023, **4**, 932–939.

10 Y. Liu, K. Ma, R. Li, X. Ren and T. S. Huang, *Cellulose*, 2013, **20**, 3123–3130.

11 S. Roest, H. C. van der Mei, T. J. A. Loontjens and H. J. Busscher, *Appl. Surf. Sci.*, 2015, **356**, 325–332.

12 A. Frei, A. D. Verderosa, A. G. Elliott, J. Zuegg and M. A. T. Blaskovich, *Nat. Rev. Chem.*, 2023, **7**, 202–224.

13 C. N. Morrison, K. E. Prosser, R. W. Stokes, A. Cordes, N. Metzler-Nolte and S. M. Cohen, *Chem. Sci.*, 2020, **11**, 1216–1225.

14 E. Sánchez-López, D. Gomes, G. Esteruelas, L. Bonilla, A. L. Lopez-Machado, R. Galindo, A. Cano, M. Espina, M. Ettcheto, A. Camins, A. M. Silva, A. Durazzo, A. Santini, M. L. Garcia and E. B. Souto, *Nanomaterials*, 2020, **10**, 292.

15 A. I. Ribeiro, A. M. Dias and A. Zille, *ACS Appl. Nano Mater.*, 2022, **5**, 3030–3064.

16 L. Windler, M. Height and B. Nowack, *Environ. Int.*, 2013, **53**, 62–73.

17 K. Gold, B. Slay, M. Knackstedt and A. K. Gaharwar, *Adv. Ther.*, 2018, **1**, 1700033.

18 P. Dhandapani, A. S. Siddarth, S. Kamalasekaran, S. Maruthamuthu and G. Rajagopal, *Carbohydr. Polym.*, 2014, **103**, 448–455.

19 N. Vigneshwaran, S. Kumar, A. A. Kathe, P. V. Varadarajan and V. Prasad, *Nanotechnology*, 2006, **17**, 5087–5095.

20 Y. Chen, Y. Zhang, H. Zhang, J. Liu and C. Song, *Chem. Eng. J.*, 2013, **228**, 12–20.

21 A. M. Gallardo-Moreno, M. A. Pacha-Olivenza, M. C. Fernández-Calderón, C. Pérez-Giraldo, J. M. Bruque and M. L. González-Martín, *Biomaterials*, 2010, **31**, 5159–5168.

22 S. Shankar, M. Lahav and M. E. van der Boom, *J. Am. Chem. Soc.*, 2015, **137**, 4050–4053.

23 T. Mosmann, *J. Immunol. Methods*, 1983, **65**, 55–63.

24 N. E.-S. Ibrahim, *Nat. Rev. Bioengg.*, 2023, **1**, 159.

25 J. Qian, Q. Dong, K. Chun, D. Zhu, X. Zhang, Y. Mao, J. N. Culver, S. Tai, J. R. German, D. P. Dean, J. T. Miller, L. Wang, T. Wu, T. Li, A. H. Brozena, R. M. Briber, D. K. Milton, W. E. Bentley and L. Hu, *Nat. Nanotechnol.*, 2023, **18**, 168–176.

26 N. Kari, S. Afroj, K. Lloyd, L. C. Oaten, D. V. Andreeva, C. Carr, A. D. Farmery, I.-D. Kim and K. S. Novoselov, *ACS Nano*, 2020, **14**, 12313–12340.

27 A. G. Hassabo, M. E. El-Naggar, A. L. Mohamed and A. A. Hebeish, *Carbohydr. Polym.*, 2019, **210**, 144–156.

28 M. Cloutier, D. Mantovani and F. Rosei, *Trends Biotechnol.*, 2015, **33**, 637–652.

29 B. Balasubramaniam, Prateek, S. Ranjan, M. Saraf, P. Kar, S. P. Singh, V. K. Thakur, A. Singh and R. K. Gupta, *ACS Pharmacol. Transl. Sci.*, 2021, **4**, 8–54.

30 K. Wu, H. Li, X. Cui and R. Feng, *et al.*, *Antimicrob. Agents Chemother.*, 2022, **66**, e0062822.

31 S. Silver, *FEMS Microbiol. Rev.*, 2003, **27**, 341–353.

32 E. Lkrewi, C. P. Randall, N. Ooi, J. L. Cottell and A. J. O'Neill, *J. Antimicrob. Chemother.*, 2017, **72**, 3043–3046.

33 H. Wang, J. Li, C. Min, F. Xia, M. Tang, J. Li, Y. Hu and M. Zou, *Infect. Drug Resist.*, 2022, **15**, 1425–1437.

34 U. Theuretzbacher, *Nat. Microbiol.*, 2020, **5**, 984–985.

35 Z. Si, K. Pethe and M. B. Chan-Park, *JACS Au*, 2023, **3**, 276–292.

36 R. Namivandi-Zangeneh, E. H. H. Wong and C. Boyer, *ACS Infect. Dis.*, 2021, **7**, 215–253.

37 J. Zhang, Y. P. Chen, K. P. Miller, M. S. Ganewatta, M. Bam, Y. Yan, M. Nagarkatti, A. W. Decho and C. Tang, *J. Am. Chem. Soc.*, 2014, **136**, 4873–4876.

38 P. Pageni, P. Yang, Y. P. Chen, Y. Huang, M. Bam, T. Zhu, M. Nagarkatti, B. C. Benicewicz, A. W. Decho and C. Tang, *Biomacromolecules*, 2018, **19**, 417–425.

39 I. Mukkatt, A. P. Mohanachandran, A. Nirmala, D. Patra and P. A. Sukumaran, *ACS Appl. Mater. Interfaces*, 2022, **14**, 31900–31910.

40 M. Indulekha, N. Anjali, N. D. Madhavan, S. Shankar, B. Deb and A. Ajayaghosh, *ACS Appl. Mater. Interfaces*, 2021, **13**, 5245–5255.

41 N. Anjali, M. Indulekha, S. Shankar and A. Ajayaghosh, *Angew. Chem., Int. Ed.*, 2021, **60**, 455–465.

42 M. Indulekha, N. Anjali, R. B. Rakhi, S. Shankar and A. Ajayaghosh, *Mater. Today Chem.*, 2020, **16**, 100260.

43 N. Elool Dov, S. Shankar, D. Cohen, T. Bendikov, K. Rehav, L. Shimon, M. Lahav and M. E. van der Boom, *J. Am. Chem. Soc.*, 2017, **139**, 11471–11481.

44 R. Balgley, S. Shankar, M. Lahav and M. E. van der Boom, *Angew. Chem., Int. Ed.*, 2015, **54**, 12457–12462.

45 S. Shankar, M. Lahav and M. E. van der Boom, *J. Am. Chem. Soc.*, 2015, **137**, 4050–4054.

46 N. Mat Zain, A. G. F. Stapley and G. Shama, *Carbohydr. Polym.*, 2014, **112**, 195–202.

47 M. Valodkar, S. Modi, A. Pal and S. Thakore, *Mater. Res. Bull.*, 2011, **46**, 384–389.

48 A. Kubacka, M. S. Diez, D. Rojo, R. Bargiela, S. Ciordia, I. Zapico, J. P. Albar, C. Barbas, V. A. P. M. dos Santos, M. Fernández-García and M. Ferrer, *Sci. Rep.*, 2014, **4**, 4134.

49 J. Shi, J. Li, Y. Wang and C. Y. Zhang, *Chem. Eng. J.*, 2022, **431**, 133714.

50 A. B. Younis, Y. Haddad, L. Kosaristanova and K. Smerkova, *Wiley Interdiscip. Rev.: Nanomed. Nanobiotechnol.*, 2023, **15**, e1860.

51 M. L. Ermini and V. Voliani, *ACS Nano*, 2021, **15**, 6008–6029.

52 B. Skóra, U. Krajewska, A. Nowak, A. Dziedzic, A. Barylyak and M. Kus-Liśkiewicz, *Sci. Rep.*, 2021, **11**, 13451.

53 L. H. Kwong, R. Wilson, S. Kumar, Y. S. Crider, Y. R. Sanchez, D. Rempel and A. Pillarisetti, *ACS Nano*, 2021, **15**, 5904–5924.

54 A. Tcharkhtchi, N. Abbasnezhad, M. Zarbini Seydani, N. Zirak, S. Farzaneh and M. Shirinbayan, *Bioactive Mater.*, 2021, **6**, 106–122.

55 J. T. J. Ju, L. N. Boisvert and Y. Y. Zuo, *Adv. Colloid Interface Sci.*, 2021, **292**, 102435.

56 Y. Wu, Y. Yang, Z. Zhang, Z. Wang, Y. Zhao and L. Sun, *Text. Res. J.*, 2019, **89**, 8677–8880.

57 Y. He, M. Wan, Z. Wang, X. Zhang, Y. Zhao and L. Sun, *Surf. Coat. Technol.*, 2019, **378**, 125079.

58 J. Cui, M. Wan, Z. Wang, Y. Zhao and L. Sun, *Sep. Purif. Technol.*, 2023, **321**, 124270.